Ornithine Decarboxylase in Macrophages Exacerbates Colitis and Promotes Colitis-Associated Colon Carcinogenesis by Impairing M1 Immune Responses

Kshipra Singh[1,4], **Lori A. Coburn**[1,4,5], **Mohammad Asim**[1], **Daniel P. Barry**[1], **Margaret M. Allaman**[1], **Chanjuan Shi**[2,3], **M. Kay Washington**[2,3], **Paula B. Luis**[6], **Claus Schneider**[4,6], **Alberto G. Delgado**[1], **M. Blanca Piazuelo**[1,4], **John L. Cleveland**[7], **Alain P. Gobert**[1,4], and **Keith T. Wilson**[1,2,3,4,5]

[1]Division of Gastroenterology, Hepatology, and Nutrition, Department of Medicine, Vanderbilt University Medical Center, Nashville, Tennessee

[2]Department of Pathology, Microbiology, and Immunology, Vanderbilt University Medical Center, Nashville, Tennessee

[3]Vanderbilt Ingram Cancer Center, Vanderbilt University Medical Center, Nashville, Tennessee

[4]Center for Mucosal Inflammation and Cancer, Vanderbilt University Medical Center, Nashville, Tennessee

[5]Veterans Affairs Tennessee Valley Healthcare System, Nashville, Tennessee

[6]Department of Pharmacology, Vanderbilt University School of Medicine, Nashville, Tennessee

[7]Department of Tumor Biology, Moffitt Cancer Center and Research Institute, Tampa, Florida

Abstract

Ornithine decarboxylase (ODC) is the rate-limiting enzyme for polyamine biosynthesis and restricts M1 macrophage activation in gastrointestinal (GI) infections. However, the role of macrophage ODC in colonic epithelial-driven inflammation is unknown. Here we investigate cell-specific effects of ODC in colitis and colitis-associated carcinogenesis (CAC). Human colonic macrophages expressed increased ODC levels in active ulcerative colitis and Crohn's disease, colitis-associated dysplasia, and CAC. Mice lacking *Odc* in myeloid cells (*Odc* [mye] mice) that

Corresponding Author: Keith T. Wilson, Division of Gastroenterology, Hepatology and Nutrition, Vanderbilt University Medical Center, 1030C Medical Research Building IV, 2215B Garland Avenue, Nashville, TN 37232, USA. Tel: 615-343-5675; Fax: 615-343-6229; keith.wilson@vanderbilt.edu.

were treated with dextran sulfate sodium (DSS) exhibited improved survival, body weight, and colon length and reduced histologic injury versus control mice. In contrast, gastrointestinal epithelial-specific *Odc* knockout had no effect on clinical parameters. Despite reduced histologic damage, colitis tissues of *Odc* [mye] mice had increased levels of multiple pro-inflammatory cytokines and chemokines and enhanced expression of M1, but not M2 markers. In the azoxymethane (AOM)-DSS model of CAC, *Odc* [mye] mice had reduced tumor number, burden, and high-grade dysplasia. Tumors from *Odc* [mye] mice had increased M1, but not M2 macrophages. Increased levels of histone 3, lysine 9 acetylation (H3K9ac), a marker of open chromatin, were manifest in tumor macrophages of *Odc* [mye] mice, consistent with our findings that macrophage ODC affects histone modifications that upregulate M1 gene transcription during GI infections. These findings support the concept that macrophage ODC augments epithelial injury-associated colitis and CAC by impairing the M1 responses that stimulate epithelial repair, antimicrobial defense, and anti-tumoral immunity. They also suggest that macrophage ODC is an important target for colon cancer chemoprevention.

Keywords

Macrophage; Ornithine decarboxylase; Colitis; Colon cancer; AOM-DSS

Introduction

M1 macrophage activation is essential in the host defense response to microbes and to tumor cells (1, 2). M2 macrophages have a key role in parasite defense, and are associated with wound healing (3). There has been a long interest in the role of M1 versus M2 macrophages in the tumor microenvironment (2, 4), but as yet this has not led to therapeutic interventions.

In inflammatory bowel disease (IBD), there is a strong risk for colitis-associated carcinogenesis (CAC) that results from the chronic inflammatory state (5, 6). Indeed, CAC occurs in 20% of patients with IBD, and mortality rates can exceed 50% (7, 8). However, despite this clinical problem, the mainstay of clinical management is annual surveillance colonoscopy. Accordingly, insight into the pathogenesis of CAC, and new therapeutic strategies, are urgently needed. In particular, the role of the host immune response in CAC, and especially the roles of M1 and M2 macrophages are not understood.

We have investigated the role of macrophage activation patterns, often referred to M1 versus M2 polarization, in host-pathogen interactions in the GI mucosa (1, 9, 10). One key regulatory component of macrophage function revealed by these studies has been the role of polyamines (10, 11). Polyamine biosynthesis begins with the production of the biogenic amine, putrescine, which is produced by the enzyme ornithine decarboxylase (ODC1, hereafter ODC) (12, 13). Putrescine is then converted to the polyamines spermidine and spermine by the action of constitutively active synthases (13). We recently reported that the myeloid-specific deletion of *Odc* (*Odc* [mye]) provokes a marked increase in the response of mouse bone marrow-derived macrophages to M1 stimuli including *Helicobacter pylori*, *Citrobacter rodentium*, or LPS + IFN-γ, and to increased expression of M1 genes (10). In addition, in mouse models of gastric inflammation induced by *H. pylori* infection, and of

colon inflammation induced by *C. rodentium* infection, *Odc* [mye] mice have increased M1 responses and production of M1 cytokines and chemokines. However, when such bone marrow-derived *Odc* [mye] macrophages are exposed to M2 stimulation with IL-4, there is also an upregulation of M2 gene expression (10). Thus, the ODC-polyamine circuit can harness both M1 and M2 macrophage responses. Finally, these effects were linked to histone modifications (10), where *Odc* [mye] macrophages have increases in histone marks that are hallmarks of open chromatin (e.g. H3K4 monomethylation and H3K9 acetylation), leading to increased transcription (10, 14).

Macrophage-driven innate immune responses are major contributors to the pathogenesis of human ulcerative colitis (UC) (15-17) and to related mouse models of colitis and CAC (1, 16, 18). Given this, we assessed the role of ODC in UC and CAC. Herein, we report that ODC expression is increased in human macrophages of IBD tissues displaying active colitis, dysplasia, and CAC. Strikingly, in both dextran sulfate sodium (DSS)-induced colitis and the azoxymethane (AOM)-DSS model of CAC, myeloid-selective loss of *Odc* reduces clinical disease and tumorigenesis, and this is linked to increases in the M1 response. Thus, in both an epithelial injury model and in associated carcinogenesis, M1 macrophage functions are beneficial, and ODC acts to impair this response, providing new insights into strategies for colon cancer prevention.

Materials and Methods

Animal studies

Animal experiments were approved by the Vanderbilt University IACUC and the Research and Development Committee of the Veterans Affairs Tennessee Valley Healthcare System. *Odc*^{fl/fl} mice, and *Odc* [mye] mice generated by crossing *Odc*^{fl/fl} with *Lyz2*[cre/cre] mice, were previously described (10). *Odc* [epi] mice were generated by crossing *Odc*^{fl/fl} mice with *Foxa3*[cre/+] mice (19, 20). Male mice between the ages of 7 and 12 weeks were used for all studies.

For the acute DSS colitis model, animals were treated with 2.5% DSS in the drinking water for 5 days followed by a 5-day recovery period. Control mice received normal drinking water for 10 days. For the colitis-associated cancer (CAC) model, mice first received one intraperitoneal injection of AOM (12.5 mg/kg) and were then treated three times with 4% DSS for 5 days beginning at days 5, 26, and 47, all as described (20).

Animals were monitored daily and mice that showed extreme distress, became moribund, or lost more than 20% of initial body weight were euthanized. After sacrifice, colons were removed, measured, cut longitudinally, cleaned, weighed, and Swiss-rolled for histology. Two proximal and distal 2 mm pieces were used for RNA and protein extraction. All histologic assessments were made in a blinded manner by a pathologist (M.K.W.). In the AOM-DSS model, tumors were counted and measured under a dissecting microscope; tumor and non-tumor tissues were collected for RNA and protein extraction. Colons were then Swiss-rolled for histology.

Isolation of myeloid cells and RNA analyses

RNA from colonic tissues was extracted using the RNeasy Mini Kit (Qiagen) (21). CD11b^{+}, CD11c^{+}, F4/80^{+} and Gr1^{+} cells were positively selected (21) using biotinylated antibodies, streptavadin conjugated with magnetic beads, and IMagnet columns (BD Biosciences). RNA from cells was isolated using the 5 PRIME PerfectPure RNA 96 Cell CS kit (21). Total RNA (1 μg) was reverse transcribed using an iScript cDNA synthesis kit (Bio-Rad) and oligo(dT) primers. Each real-time RT-PCR was performed with 2 μl of cDNA, iQ™ SYBR Green Supermix (Bio-Rad), and primers in Supplementary Table 1.

Immunofluorescence and Immunohistochemistry

Sections (5 μm) from formalin-fixed paraffin-embedded Swiss-rolled murine tissues were deparaffinized and treated with citrate buffer for antigen retrieval. An IBD-associated cancer tissue microarray (TMA) from Vanderbilt University Medical Center, which contained cases of normal tissue, inactive and active ulcerative colitis and Crohn's disease, dysplasia, and CAC, was used to assess ODC expression. Immunofluorescence for CD68, ODC, nitric oxide synthase 2 (NOS2), arginase 1 (ARG1), and H3K9Ac, and immunohistochemistry for CD8 and FOXP3 was performed as described (1, 10). Antibodies are listed in Supplementary Table 2. Quantification of immunofluorescence was performed on images generated by the Aperio Versa platform (Leica Biosystems) of the Vanderbilt Digital Histology Shared Resource using CellProfiler software (1, 20).

Measurement of cytokine and chemokines

Colonic tissues were lysed in Cell Lytic Mammalian Tissue Lysis Extraction Reagent (Sigma) and analyzed using the 25-analyte MILLIPLEX MAP Mouse Cytokine/Chemokine Magnetic Bead Panel (EMD Millipore) on a FLEXMAP 3D instrument (Luminex) (21, 22). Data were standardized to tissue protein concentrations measured by the BCA Protein Assay Kit (Pierce). TNF-α and IFN-γ in tissues was measured using R&D DuoSet ELISA kits (10).

Flow cytometry

Immune cells from non-tumor and tumor areas were isolated using Liberase DL and TL (23). Cells were stained for CD11b (Supplementary Table 2), washed, fixed, and permeabilized with CytoFix/CytoPerm (BD Biosciences). NOS2 or ARG1 antibodies were used (Supplementary Table 2). Data acquisition was performed using FlowJo software (Tree Star).

Macrophage differentiation and measurement of polyamines

Bone-marrow-derived macrophages (BMmacs) were differentiated, placed in DMEM supplemented with 2% BSA, and activated with IFN-γ (200 units/ml) and LPS (10 ng/ml) for 24 h (10). Polyamines were quantified by LC-MS in cell pellets (10).

Statistics

Data are shown as the mean ± SEM. Statistical analyses were performed with Prism version 5.0c (GraphPad Software). Student's *t* test was performed for comparison between two

groups. ANOVA with the Student-Newman-Keuls post-hoc multiple comparisons test was performed to compare multiple groups. When data were not normally distributed, log transformation was performed. Survival was analyzed by the Log-rank (Mantel-Cox) test.

Results

Patients with active UC and CAC have increased ODC expression in macrophages

To assess macrophage infiltration and ODC expression in patients with UC, as well as precancerous and cancerous colon lesions, a TMA from Vanderbilt University Medical Center was utilized. Histopathologic diagnoses were established from clinical case material from surgical resections, and confirmed by H&E staining of the cores on the TMA. Immunofluorescent staining was performed for the macrophage marker CD68, as well as ODC. Notably, this demonstrated that high levels of ODC are expressed in macrophages found in active colitis, dysplasia, and carcinoma (Fig. 1A). When scored by whole slide scanning and CellProfiler image analysis, there were marked increases in the percentage of CD68$^+$ODC$^+$ cells per core (Fig. 1B), as well as an increase in the percentage of CD68$^+$ODC$^+$ cells per CD68$^+$ cells (Fig. 1C) in the colon of patients with active colitis, dysplasia, and CAC compared to tissues from normal individuals or to tissues from inactive UC. ODC staining was also detected in epithelial cells; however, there was no significant increase in ODC levels in CD68$^-$ cells in colitis, dysplasia, or CAC (Supplementary Fig. S1A). CD68$^+$ODC$^+$ cells were also increased in active Crohn's disease tissues (Supplementary Fig. S1B and S1C). Thus, ODC is selectively overexpressed in macrophages during colonic inflammation in IBD, and in patients with pre-cancerous and cancerous lesions.

Macrophage ODC contributes to DSS-induced colonic inflammation

To investigate the relative contribution of ODC in macrophages and epithelial cells to UC and CAC, we used validated mouse experimental colitis and CAC models. *Odc* expression was elevated in colonic tissues of mice with DSS-induced colitis, and AOM-DSS-induced CAC lesions (Supplementary Fig. S2A and S2B). There was a significant increase of *Odc* mRNA levels in cells positive for the markers CD11b (myeloid cells) and F4/80 (macrophages), but not CD11c (dendritic cells) or Gr1 (neutrophils and myeloid-derived suppressor cells) from the colon of DSS-treated mice (Supplementary Fig. S2C). To further assess the role of macrophage ODC in an epithelial injury and repair model of colitis induced by DSS, we used *Odc*^{mye} (*Odc*$^{fl/fl}$;*Lyz2*$^{cre/cre}$) mice, in which we demonstrated loss of ODC in macrophages (10). At baseline, colons of *Odc*^{mye} mice are histologically normal, and do not differ from the control *Odc*$^{fl/fl}$ mice (Supplementary Fig. S3A). There were no changes in ODC expression in the epithelium of *Odc*^{mye} versus *Odc*$^{fl/fl}$ mice (Supplementary Fig. S3B). Loss of ODC activity in *Odc*^{mye} mice was verified by measuring polyamines in BMmacs. Upon stimulation with IFN-γ + LPS, BMmacs from *Odc*$^{fl/fl}$, but not *Odc*^{mye} mice, generated putrescine, the direct product of ODC; spermidine and spermine were not modulated by the M1 stimulus (Supplementary Fig. S3C). In mice treated with DSS for 5 days followed by 5 days of water, *Odc*^{mye} mice exhibited a significant improvement in survival (Fig. 2A). *Odc*$^{fl/fl}$ mice treated with DSS began to die on day 7 and by day 10, only 52% remained alive, while 88% of *Odc*^{mye} mice were alive at

day 10. Body weight loss of DSS-treated Odc^{mye} mice was also significantly improved compared to DSS-treated $Odc^{fl/fl}$ mice (Fig. 2B), and colon length was less reduced in Odc^{mye} versus $Odc^{fl/fl}$ mice (Fig. 2C). Finally, histologic colitis was significantly improved in Odc^{mye} mice compared to $Odc^{fl/fl}$ mice (Fig. 2D and 2E).

Immunofluorescence analyses established that ODC protein expression was markedly elevated in DSS-treated $Odc^{fl/fl}$ versus untreated $Odc^{fl/fl}$ mice (Fig. 2F). Further, ODC expression was predominantly in macrophages, as evidenced by co-localization to cells marked by CD68 staining (Fig. 2F, left panels). As expected, ODC staining of CD68+ cells was absent in the colon tissues of DSS-treated Odc^{mye} mice (Fig. 2F, right panels). There was modest ODC staining of CD68− colonic epithelial cells (Fig. 2F, right panels), which was not affected by myeloid-specific deletion of Odc. These data verify the specific knockout of ODC in colonic macrophages during DSS colitis.

Because ODC is also expressed in the colonic epithelial cells of UC and CAC patients, we assessed the contribution of epithelial-derived ODC to the development of DSS-induced colitis, using Odc^{epi} mice. Expression of Odc mRNA (Supplementary Fig. S4A) and ODC protein (Supplementary Fig. S4B) was abolished in colonic epithelial cells from Odc^{epi} versus $Odc^{fl/fl}$ mice. When subjected to DSS treatment, Odc^{epi} mice exhibited no differences in body weight loss, colon length, or histological injury compared to $Odc^{fl/fl}$ mice (Supplementary Fig. S4C-S4F).

ODC regulates the mucosal pro-inflammatory response during acute colitis

To gain further insights into the mechanism by which macrophage ODC contributes to the development of colitis, Luminex multiplex arrays were used to assess effects of ODC on cytokines and chemokines produced in the colonic mucosa. Despite the reduced histologic injury scores, in Odc^{mye} versus $Odc^{fl/fl}$ colon tissues from DSS-treated mice there were significant increases (Fig. 3A) in the innate cytokines CSF2 (GM-CSF), TNF-α, IL-1α, and IL-1β, as well as the prototype Th1 cytokine IFN-γ, and the chemokines CXCL2 (MIP2), CXCL9 (MIG), CXCL10 (IP-10), CCL2 (MCP-1), CCL3 (MIP-1α), CCL4 (MIP-1β), and CCL5 (RANTES). Moreover, there was increased mRNA expression of the M1 markers $Nos2$ and $Il1b$ in colitis tissues from DSS-treated Odc^{mye} mice versus DSS-treated $Odc^{fl/fl}$ mice (Fig. 3B). To further investigate the source of cytokines, macrophages were isolated by positive selection and increased mRNA expression of $Nos2$, $Tnfa$, $Il1b$, $Il12a$, $Ccl5$ and $Cxcl10$ was demonstrated in DSS-treated Odc^{mye} versus $Odc^{fl/fl}$ mice (Supplementary Fig. S5). In contrast, expression levels of the M2 markers, $Arg1$ and $Chil3$, were comparable in colonic tissues of DSS-treated $Odc^{fl/fl}$ and Odc^{mye} mice (Fig. 3B).

Odc^{mye} mice are protected from CAC

Since Odc^{mye} mice are protected in the DSS colitis model and macrophage ODC expression was detected in patients with CAC, we reasoned that macrophage ODC may play a role in colon carcinogenesis. Odc^{mye} and $Odc^{fl/fl}$ mice were subjected to the 77-day AOM-DSS model of CAC. The survival rate of Odc^{mye} mice was significantly improved compared to the $Odc^{fl/fl}$ animals on the AOM-DSS protocol (Fig. 4A). With the first and second cycles of DSS, $Odc^{fl/fl}$ and Odc^{mye} mice showed similar weight loss and recovery

with water (Fig. 4B), but with the third cycle of DSS, Odc^{mye} mice had less weight loss than $Odc^{fl/fl}$ mice, and better improvement during the recovery period (Fig. 4B). Consistent with this difference in body weights, Odc^{mye} mice had a significantly lower number of tumors per mouse (Fig. 4C) and lower overall tumor burden (Fig. 4D) than $Odc^{fl/fl}$ animals. However, there was no difference in histologic injury scores in the non-tumor area between both type of mice (Fig. 4E), most likely due to the long-time gap between the last dose of DSS and sacrifice (28 days). Histologic assessment of the tumors revealed less high-grade dysplasia in Odc^{mye} versus $Odc^{fl/fl}$ mice (Fig. 4F and 4G).

Loss of *Odc* enhances macrophage polarization towards M1 during experimental CAC

The treatment of mice with AOM-DSS led to increases in mRNA expression of the M1 markers *Nos2*, *Il1b*, *Il12a*, *Il12b*, and *Tnfa*, as well as the Th1 marker *Ifng*, in both the non-tumor and tumor areas (Fig. 5A). Strikingly, all of these markers were significantly more expressed in the tumors of the Odc^{mye} versus $Odc^{fl/fl}$ mice (Fig. 5A). TNF-α and IFN-γ levels were measured and were also increased at the protein level in tumor tissues from Odc^{mye} versus $Odc^{fl/fl}$ mice (Fig. 5B). While mRNA expression of the M2 markers *Arg1*, *Chil3*, *Tgfb*, *Vegfa*, *Il10*, and *Tnfsf14* were also generally upregulated in the non-tumor and tumor tissues, there were no significant differences in their expression between the $Odc^{fl/fl}$ and Odc^{mye} tumors (Supplementary Fig. S6).

To confirm these findings, we analyzed by flow cytometry the expression of the prototype M1 and M2 proteins, NOS2 and ARG1, respectively, in intratumoral macrophages. The numbers of NOS2+CD11b+ cells were significantly higher in tumors from Odc^{mye} mice versus tumors from $Odc^{fl/fl}$ animals (Fig. 6A), while no differences were observed in ARG1 expression in CD11b+ cells (Fig. 6A). The composite data from multiple animals demonstrated significant increases in the percentage of NOS2+CD11b+ cells (Fig. 6B), but not ARG1+CD11b+ cells (Fig. 6C), in the tumors of AOM-DSS-treated Odc^{mye} mice versus tumors from $Odc^{fl/fl}$ mice. When quantified as number of cells per gram of colon tissue, a similar pattern of increased NOS2+ (Supplementary Fig. S7A), but not ARG1+ cells (Supplementary Fig. S7B) in the CD11b+ cells was demonstrated, resulting in an increased ratio of NOS2/ARG1 in the CD11b cells (Supplementary Fig. S7C). Similarly, by immunofluorescence, the level of ARG1 in CD68+ cells was not affected by *Odc* loss (Fig. 7A), whereas NOS2 was more abundant in CD68+ cells present in the tumors of Odc^{mye} mice than in tumors of $Odc^{fl/fl}$ animals (Fig. 7B). There were no differences in staining for the Treg marker, FOXP3, or the cytotoxic T cell marker, CD8, in tumors of Odc^{mye} versus $Odc^{fl/fl}$ mice (Supplementary Fig. S8).

In GI infection models, *Odc* loss in macrophages provokes increases in histone marks that are typical of open chromatin and that are associated with the increased expression of genes encoding M1 markers (NOS2 and cytokines), as described (10). Notably, macrophage levels of the euchromatin histone mark H3K9ac, which is associated with M1 gene expression (10), were augmented in the tumors of Odc^{mye} mice versus those in $Odc^{fl/fl}$ animals (Fig. 7C).

Discussion

The findings presented herein establish critical roles for macrophage ODC in colonic inflammation and associated colon tumorigenesis. Specifically, mice with myeloid-specific knockout of *Odc* have more robust cytokine and chemokine responses, yet are protected in terms of clinical parameters and histologic injury in the DSS injury-repair model of colitis. This suggests that macrophage ODC impairs responses to the injury induced by DSS, and suggests that increased macrophage ODC expression in UC may contribute to epithelial cell injury. In contrast, intestinal epithelial cell knockout of *Odc* does not result in significant changes in the level of DSS-induced colitis. Thus, polyamines derived from ODC have macrophage-selective effects on colonic injury and repair.

Because polyamines are well known to support cell proliferation, ODC has been a target to limit carcinogenesis (24) and/or to limit tumor progression (25), including in colon cancer prevention (26). Here we found that ODC expression is increased in the colonic macrophages of mice treated with DSS, but is not overexpressed in the epithelium in this model. In colitis tissues, immunofluorescence demonstrated strong double-staining for ODC and macrophages, and positive selection studies showed that macrophages represent the myeloid subpopulation with an increase in *Odc* expression. These data indicate that macrophages are the main source of ODC during colitis, although basal ODC in other immune cells could have a role. ODC enzymatic activity has been shown to be increased in colon tissues from humans with familial or somatic *APC* mutations (27) as well as in the $Apc^{min/+}$ mouse model of genetically-driven intestinal tumorigenesis (28). However, to our knowledge, ODC has not been immunolocalized in either human colitis or colon cancer. Using a human TMA, we found that ODC protein levels are increased in colonic macrophages in patients with active ulcerative colitis, and with colitis-associated dysplasia or colon cancer, validating the relevance of our animal studies and suggesting the involvement of macrophage ODC in the pathophysiology of colitis and CAC.

In the present study, we show that *Odc* loss in myeloid cells is associated with increased levels of innate immune mediators, including multiple chemokines and cytokines that are hallmarks of M1 macrophages, as well as the Th1 cytokine IFN-γ. These results are consistent with our findings that ODC-derived polyamines inhibit macrophage activation in both *H. pylori*-induced gastritis and in *Citrobacter rodentium*-induced colitis (10), such that macrophage ODC suppresses innate immune response to infection, through effects on gene transcription, limiting gastritis and colitis in these models. The data reported herein reveal a more complex scenario, where despite increases in pro-inflammatory chemokines and cytokines that are manifest with myeloid deletion of *Odc*, the *Odc* ^{mye} animals have improved recovery, better preservation of colon structure, and reduced histologic inflammation and epithelial injury. As epithelial deletion of *Odc* does not provide benefit, these findings support the concept that activation of innate immune responses in M1 macrophages confers protection from colitis. Consistent with this model, depletion of macrophages in mice worsens experimental colitis (29).

Quite strikingly, the increased mucosal innate immune response in *Odc* ^{mye} mice impaired tumorigenesis in the colon. Despite this, there was no reduction in histologic colitis and no

difference in M1 gene expression in the non-tumor areas of the *Odc* ^{mye} versus *Odc*$^{fl/fl}$ mice. This could be due to the long recovery period after the final dose of DSS (25 days), but could also reflect the specificity of the increased M1 response against tumors. The reduction of tumorigenesis in *Odc* ^{mye} mice was somewhat unexpected, as the inflammatory response is thought to drive the development of tumors in the AOM-DSS model (20, 30), and disease duration of ulcerative colitis in humans is associated with increased risk for colonic dysplasia and carcinoma (31). Further, macrophage depletion in mice using clodronate-filled liposomes reduces tumor number and burden in the AOM-DSS model (18), whereas macrophage depletion in the DSS model augments colitis (29). Also confounding are findings that *Tlr4*$^{-/-}$ mice exhibit less mucosal immune response and less tumor development with AOM-DSS treatment (32), yet signaling through MyD88, the main downstream effector of TLR4, reduces DNA damage and tumors in the same CAC model (33). Similarly, although TNF-α has been shown to exhibit anti-cancer properties (34), mice lacking TNF-Rp55 develop less tumors than wild-type animals with AOM-DSS treatment (35).

Given the apparently paradoxical effects of myeloid *Odc* loss on CAC, we assessed the phenotype of tumor-associated macrophages. Notably, *Odc*-deficient macrophages display a robust M1 mRNA and protein response, and the M1 phenotype is known to have anti-tumor activities (36, 37), principally through the production of NOS2-derived nitric oxide (36, 38). Further, M1 cells support the development and the proliferation of Th1 cells that exhibit anti-tumor activities through the production of IFN-γ (39, 40) and inhibit Th2-mediated expression of the genotoxic factor activation-induced cytidine deaminase (41). In accordance with these features, IFN-γ expression is increased in the tumors of AOM-DSS-treated *Odc* ^{mye} versus *Odc*$^{fl/fl}$ mice. In contrast, the myeloid *Odc* deficiency does not increase the development of intratumoral M2 macrophages that promote tumorigenesis (42) by suppressing immunity via production of TGF-β (43, 44) and IL-10 (45), and by supporting angiogenesis (44, 46). While reduced clinical colitis with DSS may be relevant, our findings are consistent with a model where M1 polarization of macrophages is critical for the host to combat against carcinogenesis, and where macrophage ODC restricts M1 polarization. Further, increased M1 polarization by targeting myeloid ODC is mechanistically linked *in vivo* to changes in histone marks in tumors, and is consistent with the concept that the polyamine putrescine regulates chromatin structure and M1 target gene expression as found in infectious colitis (10). The lack of differences in tumor infiltrating T cells further points to a key role for the effect of ODC on macrophages.

In conclusion, the findings that macrophage ODC dampens the innate immune response, and M1-driven anti-tumoral immunity suggests that targeting macrophage ODC is an attractive approach to prevent development of CAC. Thus, agents that can specifically suppress ODC and/or polyamine availability in macrophages may show benefit in high-risk patients with UC-associated dysplasia or other forms of precancerous lesions, such as intestinal metaplasia associated with Barrett's esophagus and *H. pylori* infection, which also can lead to inflammatory carcinogenesis. In summary, ODC not only enhances tumor cell proliferation, but also prevents M1 macrophage-mediated anti-tumor immunity.

Supplementary Material

Refer to Web version on PubMed Central for supplementary material.

References

1. Hardbower DM, Singh K, Asim M, Verriere TG, Olivares-Villagomez D, Barry DP, et al. EGFR regulates macrophage activation and function in bacterial infection. J Clin Invest. 2016; 126:3296–312. [PubMed: 27482886]

2. Isidro RA, Appleyard CB. Colonic macrophage polarization in homeostasis, inflammation, and cancer. Am J Physiol Gastrointest Liver Physiol. 2016; 311:G59–73. [PubMed: 27229123]

3. Galvan-Pena S, O'Neill LA. Metabolic reprograming in macrophage polarization. Front Immunol. 2014; 5:420. [PubMed: 25228902]

4. Monteleone G, Pallone F, Stolfi C. The dual role of inflammation in colon carcinogenesis. Int J Mol Sci. 2012; 13:11071–84. [PubMed: 23109839]

5. Ekbom A, Helmick C, Zack M, Adami HO. Ulcerative colitis and colorectal cancer. A population-based study. N Engl J Med. 1990; 323:1228–33. [PubMed: 2215606]

6. Eaden JA, Abrams KR, Mayberry JF. The risk of colorectal cancer in ulcerative colitis: A meta-analysis. Gut. 2001; 48:526–35. [PubMed: 11247898]

7. Feagins LA, Souza RF, Spechler SJ. Carcinogenesis in BD: Potential targets for the prevention of colorectal cancer. Nat Rev Gastroenterol Hepatol. 2009; 6:297–305. [PubMed: 19404270]

8. Terzic J, Grivennikov S, Karin E, Karin M. Inflammation and colon cancer. Gastroenterology. 2010; 138:2101–14 e5. [PubMed: 20420949]

9. Gobert AP, Verriere T, Asim M, Barry DP, Piazuelo MB, de Sablet T, et al. Heme oxygenase-1 dysregulates macrophage polarization and the immune response to *Helicobacter pylori*. J Immunol. 2014; 193:3013–22. [PubMed: 25108023]

10. Hardbower DM, Asim M, Luis PB, Singh K, Barry DP, Yang C, et al. Ornithine decarboxylase regulates M1 macrophage activation and mucosal inflammation via histone modifications. Proc Natl Acad Sci U S A. 2017; 114:E751–E60. [PubMed: 28096401]

11. Gobert AP, Cheng Y, Wang JY, Boucher JL, Iyer RK, Cederbaum SD, et al. *Helicobacter pylori* induces macrophage apoptosis by activation of arginase II. J Immunol. 2002; 168:4692–700. [PubMed: 11971019]

12. Pegg AE. Regulation of ornithine decarboxylase. J Biol Chem. 2006; 281:14529–32. [PubMed: 16459331]

13. Pegg AE. Functions of polyamines in mammals. J Biol Chem. 2016; 291:14904–12. [PubMed: 27268251]

14. Venkatesh S, Workman JL. Histone exchange, chromatin structure and the regulation of transcription. Nat Rev Mol Cell Biol. 2015; 16:178–89. [PubMed: 25650798]

15. Baumgart DC, Carding SR. Inflammatory bowel disease: Cause and immunobiology. Lancet. 2007; 369:1627–40. [PubMed: 17499605]

16. Schenk M, Bouchon A, Seibold F, Mueller C. TREM-1-expressing intestinal macrophages crucially amplify chronic inflammation in experimental colitis and inflammatory bowel diseases. J Clin Invest. 2007; 117:3097–106. [PubMed: 17853946]

17. Rahman FZ, Smith AM, Hayee B, Marks DJ, Bloom SL, Segal AW. Delayed resolution of acute inflammation in ulcerative colitis is associated with elevated cytokine release downstream of TLR4. PLoS One. 2010; 5:e9891. [PubMed: 20360984]

18. Bader JE, Enos RT, Velazquez KT, Carson MS, Nagarkatti M, Nagarkatti PS, et al. Macrophage depletion using clodronate liposomes decreases tumorigenesis and alters gut microbiota in the AOM/DSS mouse model of colon cancer. Am J Physiol Gastrointest Liver Physiol. 2017 ajpgi. 00229.2017.

19. Sierra JC, Asim M, Verriere TG, Piazuelo MB, Suarez G, Romero-Gallo J, et al. Epidermal growth factor receptor inhibition downregulates *Helicobacter pylori*-induced epithelial inflammatory responses, DNA damage and gastric carcinogenesis. Gut. 2017 gutjnl-2016-312888.

20. Hardbower DM, Coburn LA, Asim M, Singh K, Sierra JC, Barry DP, et al. EGFR-mediated macrophage activation promotes colitis-associated tumorigenesis. Oncogene. 2017; 36:3807–19. [PubMed: 28263971]

21. Singh K, Coburn LA, Barry DP, Asim M, Scull BP, Allaman MM, et al. Deletion of cationic amino acid transporter 2 exacerbates dextran sulfate sodium colitis and leads to an IL-17-predominant t cell response. Am J Physiol Gastrointest Liver Physiol. 2013; 305:G225–40. [PubMed: 23703655]

22. Barry DP, Asim M, Scull BP, Piazuelo MB, de Sablet T, Lewis ND, et al. Cationic amino acid transporter 2 enhances innate immunity during *Helicobacter pylori* infection. PloS One. 2011; 6:e29046. [PubMed: 22194986]

23. Cassetta L, Noy R, Swierczak A, Sugano G, Smith H, Wiechmann L, et al. Isolation of mouse and human tumor-associated macrophages. Adv Exp Med Biol. 2016; 899:211–29. [PubMed: 27325269]

24. Alexiou GA, Lianos GD, Ragos V, Galani V, Kyritsis AP. Difluoromethylornithine in cancer: New advances. Future Oncol. 2017; 13:809–19. [PubMed: 28125906]

25. Ye C, Geng Z, Dominguez D, Chen S, Fan J, Qin L, et al. Targeting ornithine decarboxylase by alpha-difluoromethylornithine inhibits tumor growth by impairing myeloid-derived suppressor cells. J Immunol. 2016; 196:915–23. [PubMed: 26663722]

26. Meyskens FL Jr, McLaren CE, Pelot D, Fujikawa-Brooks S, Carpenter PM, Hawk E, et al. Difluoromethylornithine plus sulindac for the prevention of sporadic colorectal adenomas: A randomized placebo-controlled, double-blind trial. Cancer Prev Res (Phila). 2008; 1:32–8. [PubMed: 18841250]

27. Giardiello FM, Hamilton SR, Hylind LM, Yang VW, Tamez P, Casero RA Jr. Ornithine decarboxylase and polyamines in familial adenomatous polyposis. Cancer Res. 1997; 57:199–201. [PubMed: 9000553]

28. Erdman SH, Ignatenko NA, Powell MB, Blohm-Mangone KA, Holubec H, Guillen-Rodriguez JM, et al. *Apc*-dependent changes in expression of genes influencing polyamine metabolism, and consequences for gastrointestinal carcinogenesis, in the min mouse. Carcinogenesis. 1999; 20:1709–13. [PubMed: 10469614]

29. Qualls JE, Kaplan AM, van Rooijen N, Cohen DA. Suppression of experimental colitis by intestinal mononuclear phagocytes. J Leukoc Biol. 2006; 80:802–15. [PubMed: 16888083]

30. Barrett CW, Fingleton B, Williams A, Ning W, Fischer MA, Washington MK, et al. MTGR1 is required for tumorigenesis in the murine AOM/DSS colitis-associated carcinoma model. Cancer Res. 2011; 71:1302–12. [PubMed: 21303973]

31. Beaugerie L, Itzkowitz SH. Cancers complicating inflammatory bowel disease. N Engl J Med. 2015; 372:1441–52. [PubMed: 25853748]

32. Fukata M, Shang L, Santaolalla R, Sotolongo J, Pastorini C, Espana C, et al. Constitutive activation of epithelial TLR4 augments inflammatory responses to mucosal injury and drives colitis-associated tumorigenesis. Inflamm Bowel Dis. 2011; 17:1464–73. [PubMed: 21674704]

33. Salcedo R, Worschech A, Cardone M, Jones Y, Gyulai Z, Dai RM, et al. MyD88-mediated signaling prevents development of adenocarcinomas of the colon: Role of interleukin 18. J Exp Med. 2010; 207:1625–36. [PubMed: 20624890]

34. Drutskaya MS, Efimov GA, Kruglov AA, Kuprash DV, Nedospasov SA. Tumor necrosis factor, lymphotoxin and cancer. IUBMB Life. 2010; 62:283–9. [PubMed: 20155809]

35. Popivanova BK, Kitamura K, Wu Y, Kondo T, Kagaya T, Kaneko S, et al. Blocking TNF-alpha in mice reduces colorectal carcinogenesis associated with chronic colitis. J Clin Invest. 2008; 118:560–70. [PubMed: 18219394]

36. Edin S, Wikberg ML, Dahlin AM, Rutegard J, Oberg A, Oldenborg PA, et al. The distribution of macrophages with a M1 or M2 phenotype in relation to prognosis and the molecular characteristics of colorectal cancer. PLoS One. 2012; 7:e47045. [PubMed: 23077543]

37. Ryan AE, Colleran A, O'Gorman A, O'Flynn L, Pindjacova J, Lohan P, et al. Targeting colon cancer cell NF-kappaB promotes an anti-tumour M1-like macrophage phenotype and inhibits peritoneal metastasis. Oncogene. 2015; 34:1563–74. [PubMed: 24704833]

38. Scott DJ, Hull MA, Cartwright EJ, Lam WK, Tisbury A, Poulsom R, et al. Lack of inducible nitric oxide synthase promotes intestinal tumorigenesis in the *Apc(Min/+)* mouse. Gastroenterology. 2001; 121:889–99. [PubMed: 11606502]

39. Dunn GP, Koebel CM, Schreiber RD. Interferons, immunity and cancer immunoediting. Nat Rev Immunol. 2006; 6:836–48. [PubMed: 17063185]

40. Osawa E, Nakajima A, Fujisawa T, Kawamura YI, Toyama-Sorimachi N, Nakagama H, et al. Predominant T helper type 2-inflammatory responses promote murine colon cancers. Int J Cancer. 2006; 118:2232–6. [PubMed: 16331625]

41. Endo Y, Marusawa H, Kou T, Nakase H, Fujii S, Fujimori T, et al. Activation-induced cytidine deaminase links between inflammation and the development of colitis-associated colorectal cancers. Gastroenterology. 2008; 135:889–98. 98 e1–3. [PubMed: 18691581]

42. Wang W, Li X, Zheng D, Zhang D, Peng X, Zhang X, et al. Dynamic changes and functions of macrophages and M1/M2 subpopulations during ulcerative colitis-associated carcinogenesis in an AOM/DSS mouse model. Mol Med Rep. 2015; 11:2397–406. [PubMed: 25434400]

43. Hahm KB, Lee KM, Kim YB, Hong WS, Lee WH, Han SU, et al. Conditional loss of TGF-beta signalling leads to increased susceptibility to gastrointestinal carcinogenesis in mice. Aliment Pharmacol Ther. 2002; 16(Suppl 2):115–27.

44. Novitskiy SV, Pickup MW, Chytil A, Polosukhina D, Owens P, Moses HL. Deletion of TGF-beta signaling in myeloid cells enhances their anti-tumorigenic properties. J Leukoc Biol. 2012; 92:641–51. [PubMed: 22685318]

45. Berg DJ, Davidson N, Kuhn R, Muller W, Menon S, Holland G, et al. Enterocolitis and colon cancer in interleukin-10-deficient mice are associated with aberrant cytokine production and CD4(+) Th1-like responses. J Clin Invest. 1996; 98:1010–20. [PubMed: 8770874]

46. Pickert G, Lim HY, Weigert A, Haussler A, Myrczek T, Waldner M, et al. Inhibition of GTP cyclohydrolase attenuates tumor growth by reducing angiogenesis and M2-like polarization of tumor associated macrophages. Int J Cancer. 2013; 132:591–604. [PubMed: 22753274]

Significance

Ornithine decarboxylase contributes to the pathogenesis of colitis and associated carcinogenesis by impairing M1 macrophage responses needed for anti-tumoral immunity; targeting ODC in macrophages may represent a new strategy for chemoprevention.
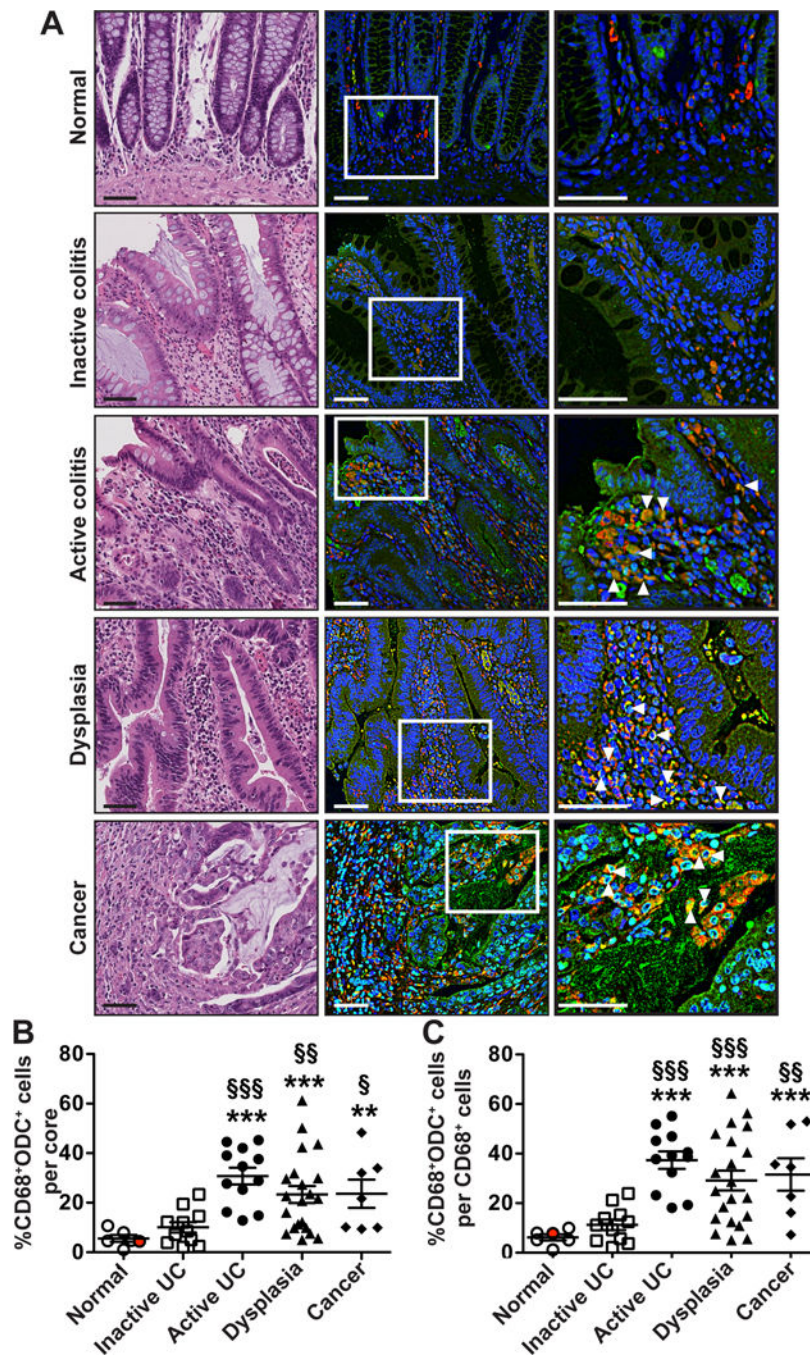
Figure 1.

Staining of human colon TMA. **A**, Representative H&E staining and immunofluorescence for CD68 (red), ODC (green), and nuclei (DAPI, blue) in the TMA; CD68+ODC+ cells are depicted in yellow in these merged images. Normal subjects: 5 tissues were from the uninvolved normal area (open circles) and 1 tissue (red circle) was from a normal control case. Boxes indicate areas of the images shown in higher magnification. Arrowheads denote cells double-positive for CD68 and ODC. Scale bars, 50 μm. **B-C**, Quantification of CD68+ODC+ cells among the total number of cells in each individual core (**B**), or among the

total number of CD68^{+} cells in each individual core (**C**) was determined using CellProfiler software. For **B** and **C**, **$P < 0.01$ and ***$P < 0.001$ versus Normal; §$P < 0.05$, §§$P < 0.01$, §§§$P < 0.001$ compared to inactive colitis.
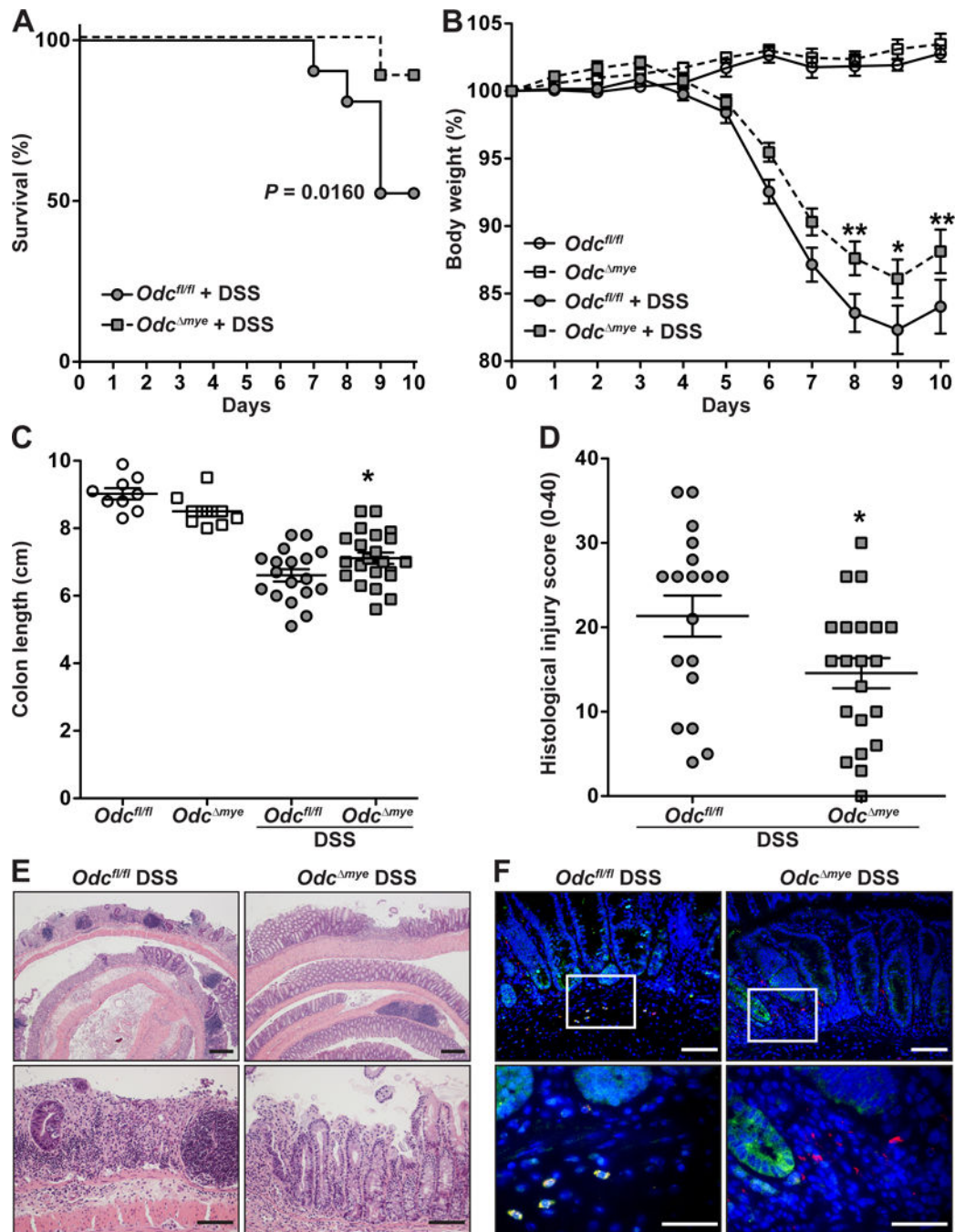
Figure 2.

Effect of myeloid-specific *Odc* deletion on DSS-induced colitis. Mice were treated with 2.5% DSS for 5 days and given normal drinking water for the next 5 days. **A**, Survival was monitored daily. The Kaplan–Meier plot was generated from 2 separate experiments pooled together; $n = 22$ *Odc*$^{fl/fl}$ mice and $n = 22$ *Odc*^{mye} mice. For this representation of the data, survival is defined as body weight loss of more than 20%. No death was observed in untreated animals. **B**, Body weights, presented as the percentage of initial body weight. *$P <$ 0.05, **$P <$ 0.01 compared to DSS-treated *Odc*$^{fl/fl}$ animals. **C**, Colon length; *$P <$ 0.05

compared to DSS-treated *Odc*$^{fl/fl}$ mice. **D-E**, Colons were Swiss-rolled and scored for histologic injury (**D**) from tissues stained with H&E (**E**); *P< 0.05 compared to DSS-treated *Odc*$^{fl/fl}$ mice. Scale bars, 100 μm. **F**, immunofluorescence for CD68 (red), ODC (green) and nuclei (blue) in colonic tissues; CD68$^+$ODC$^+$ cells in the merged images are depicted in yellow. Scale Bar, 100 μm.
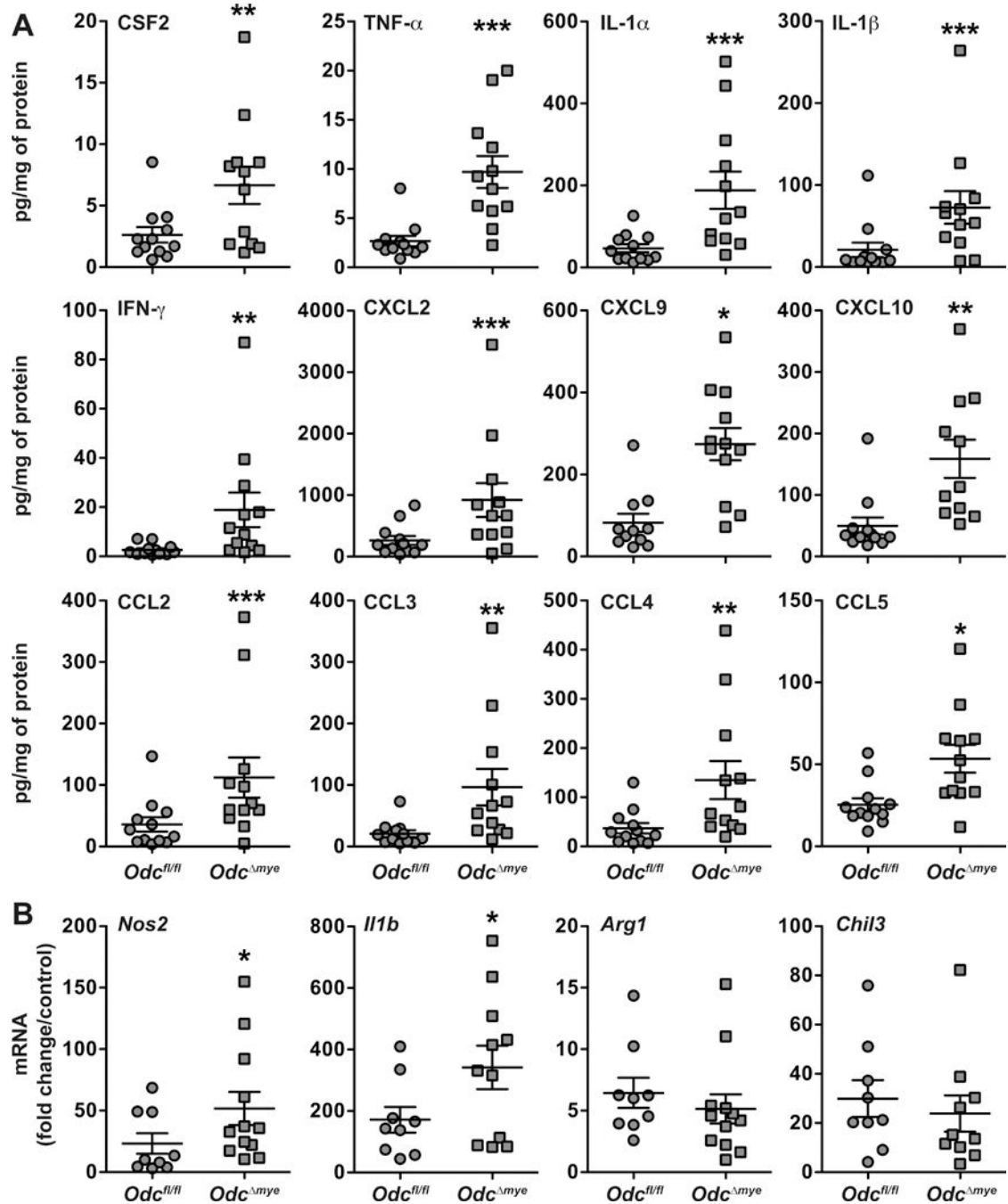
Figure 3.
Quantification of cytokines and chemokines, as well as gene expression of M1 and M2 markers in murine colonic tissues. **A**, Concentrations of cytokines and chemokines in colon tissues were determined by Luminex assay. **B**, Analysis of *Nos2*, *Il1b*, *Arg1*, and *Chil3* mRNA expression in colonic tissues. In **A** and **B**, *$P< 0.05$, **$P< 0.01$, and ***$P< 0.001$ versus *Odc^{fl/fl}* mice.
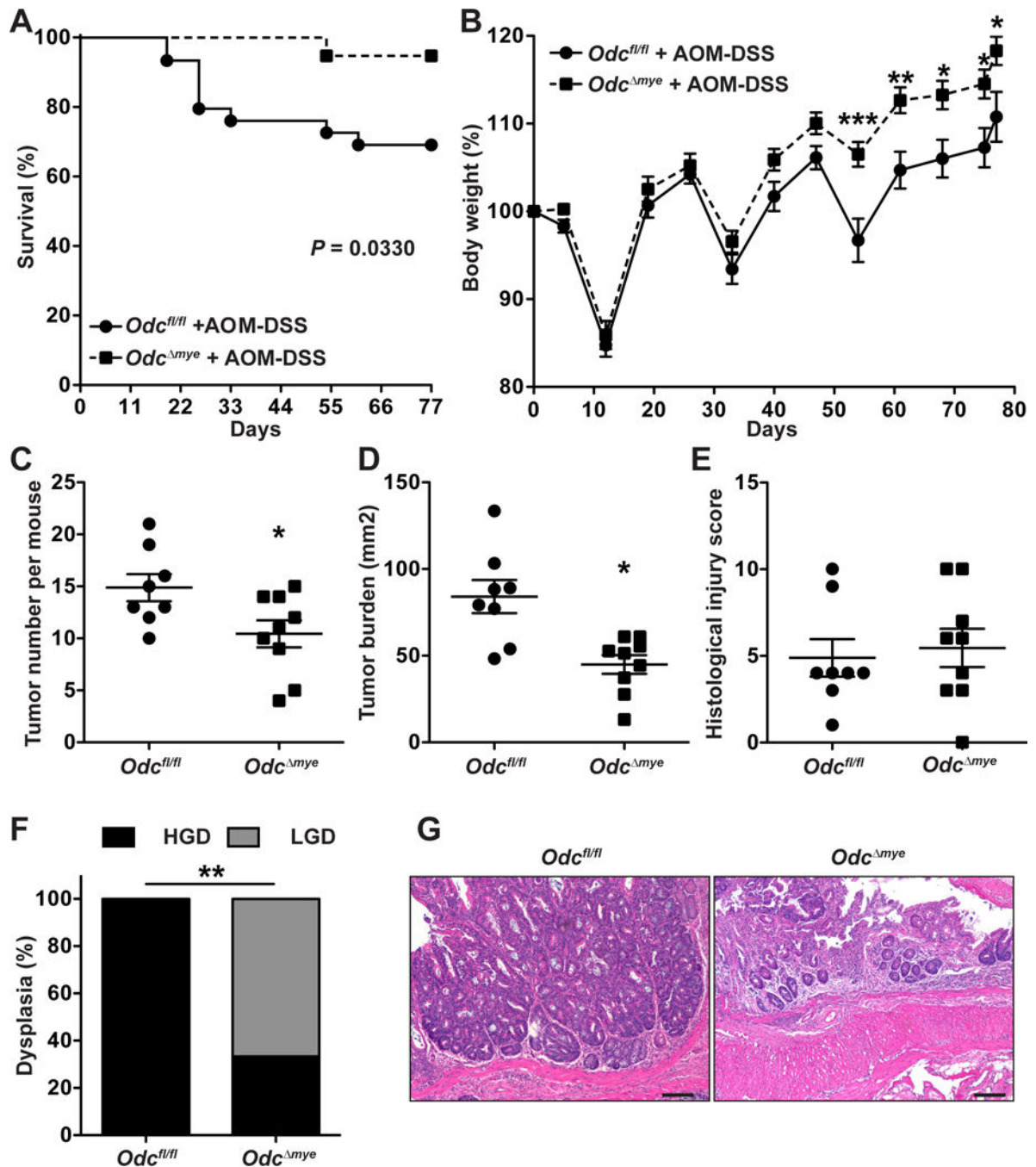
Figure 4.
Effect of myeloid-specific *Odc* deletion on AOM-DSS-induced CAC. **A**, Survival was monitored daily; the Kaplan–Meier plot was performed from 2 separate experiments pooled together; $n = 14$ *Odc*^fl/fl^ mice and $n = 11$ *Odc* ^mye^ mice. No death was observed in control animals. **B**, Percentage of initial body weight was determined at the indicated time points. **C**, Tumor number, determined using a dissecting microscope. **D**, Tumor burden, determined by the addition of the area of each tumor. **E**, Histologic colitis. **F**, Percentage of cases with low-grade dysplasia (LGD) and high-grade dysplasia (HGD). **G**, Representative H&E-stained

images from AOM-DSS-treated mice. Scale bars, 100 μm. For **B**-**F**, *$P < 0.05$, **$P < 0.01$, and ***$P < 0.001$ compared to *Odc*$^{fl/fl}$ mice treated with AOM-DSS.
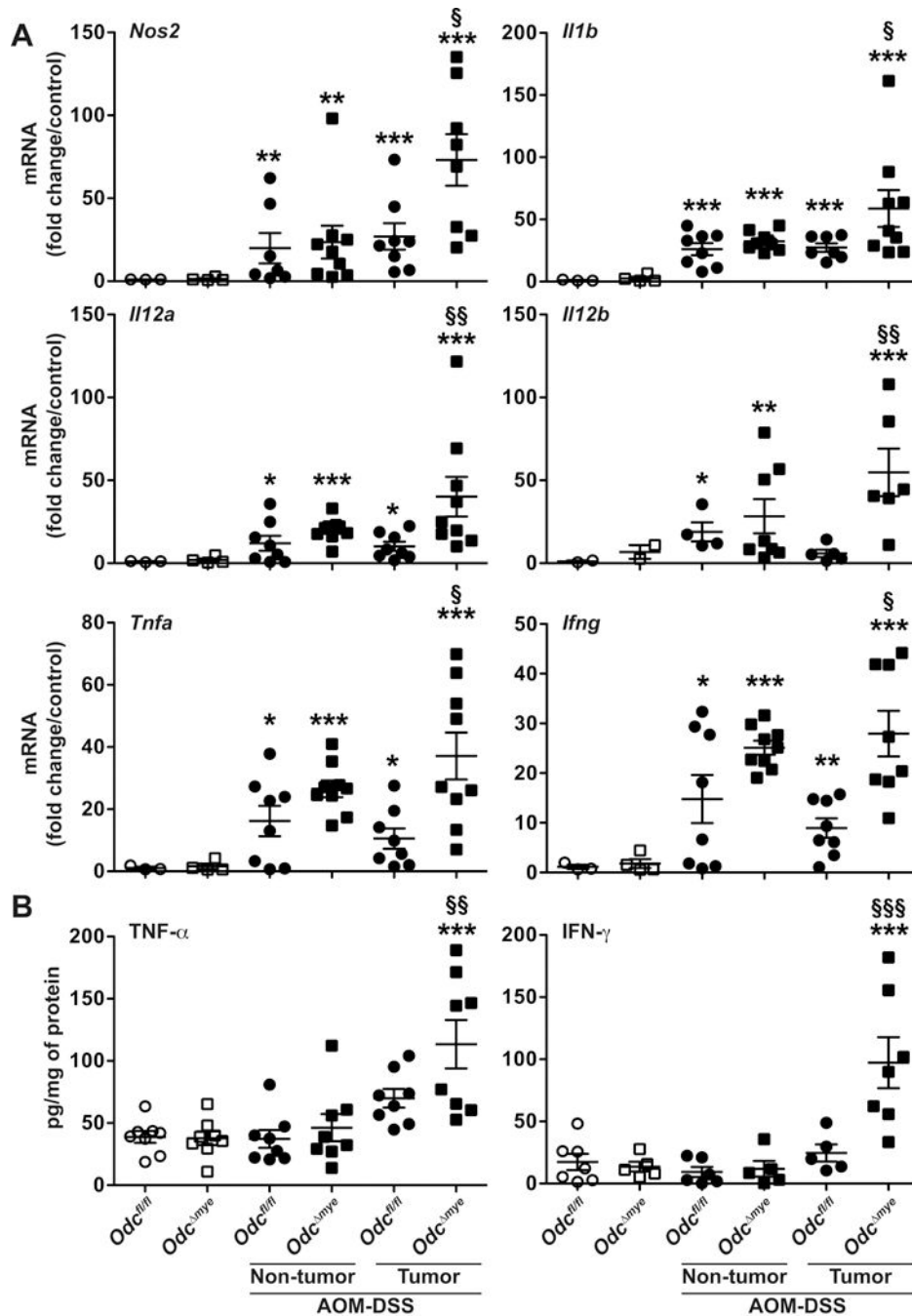
Figure 5.
M1 profile in non-tumor and tumor tissues. **A**, mRNA levels of M1 markers *Nos2*, *Il1b*, *Il12a*, *Il12b*, *Tnfa* and *Ifng* assessed by real-time RT-PCR and **B**, TNF-α and IFN-γ were also analyzed by ELISA from colonic tissues 77 days post-AOM injection. *$P < 0.05$, **$P < 0.01$, and **$P < 0.001$ compared to untreated *Odc$^{fl/fl}$* mice; §$P < 0.05$, §§$P < 0.01$, §§§$P < 0.001$ compared to the tumors in *Odc$^{fl/fl}$* mice.
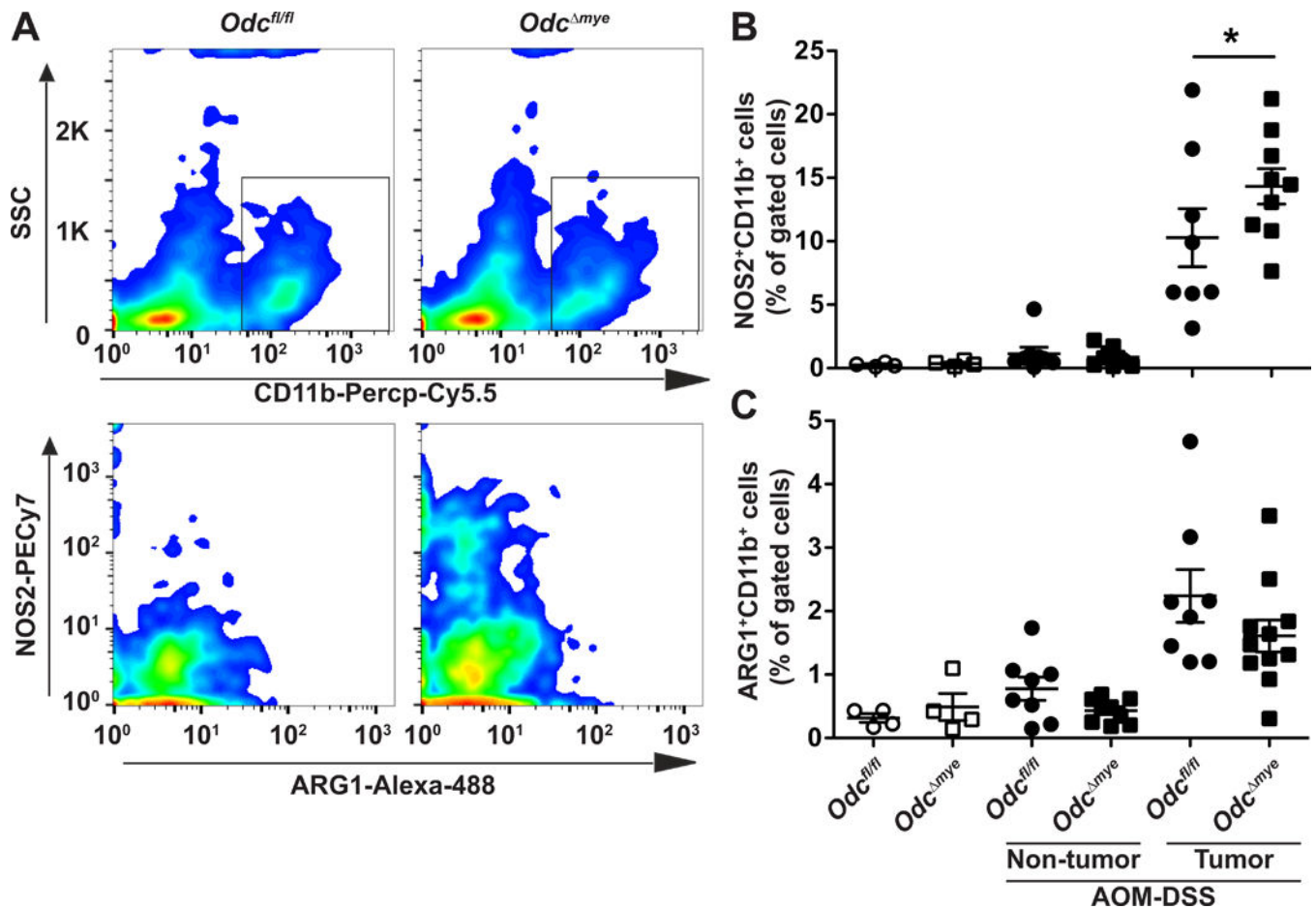
Figure 6.
Flow cytometry analysis of NOS2 and ARG1 protein expression in colon tissues from
$Odc^{fl/fl}$ and $Odc^{\Delta mye}$ mice. **A**, Representative flow plots showing NOS2 and ARG1
expression in CD11b$^+$ cells within the immune cells isolated from colon tissues of $Odc^{fl/fl}$
and $Odc^{\Delta mye}$ mice treated with AOM-DSS. **B-C**, The number of NOS2$^+$CD11b$^+$ (**B**) and
ARG1$^+$CD11b$^+$ (**C**) cells were counted and are expressed as a percent of CD11b$^+$ cells. *$P<$
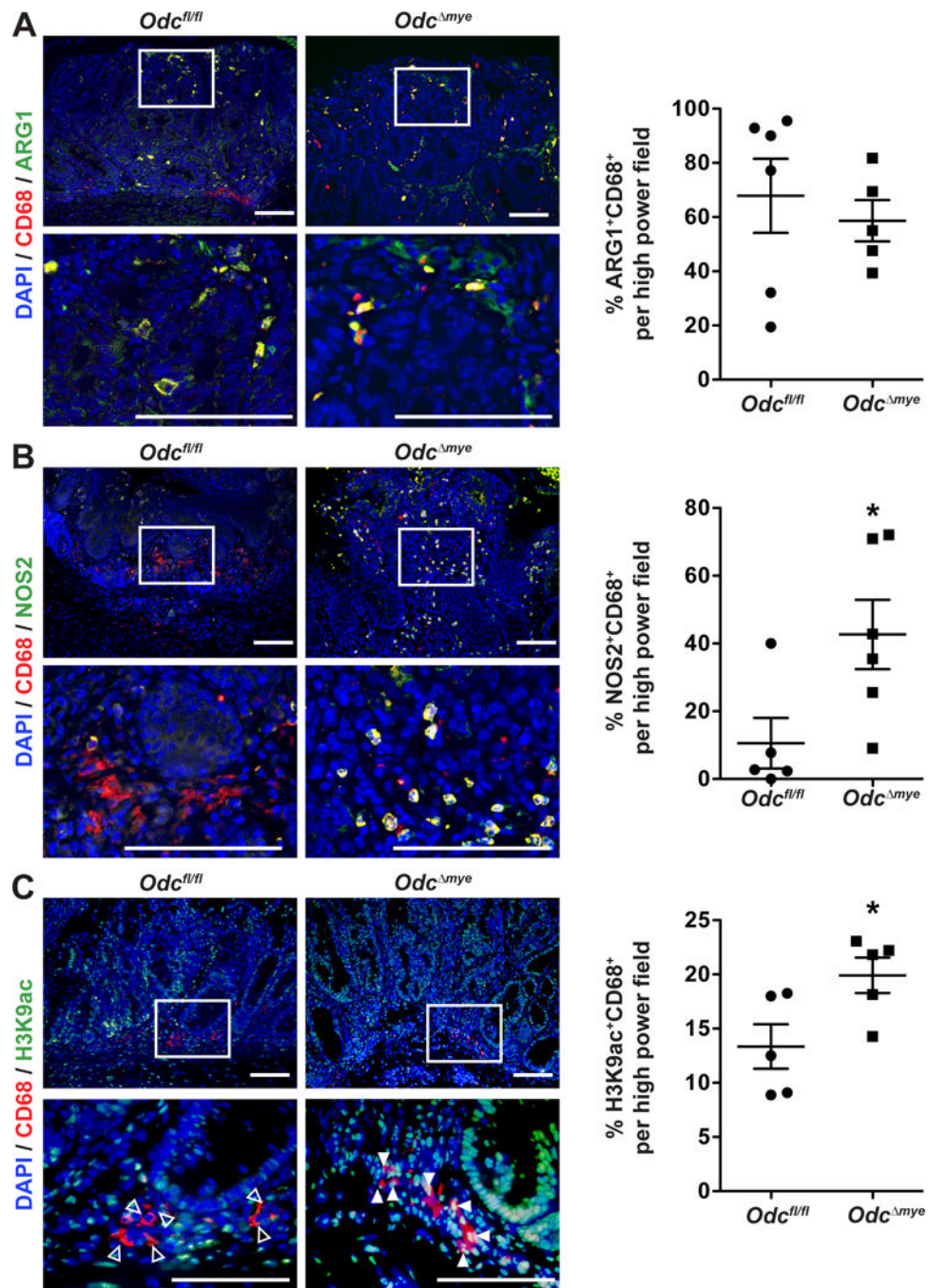0.05 versus the expression of NOS2 in tumors from $Odc^{fl/fl}$ mice.

Figure 7.
Immunofluorescent detection of ARG1, NOS2, and H3K9ac in colonic tumors from $Odc^{fl/fl}$ and $Odc^{\Delta mye}$ mice. A tumor area of the colon of AOM-DSS-treated $Odc^{fl/fl}$ and $Odc^{\Delta mye}$ mice was used to determine the levels of ARG1 (**A**), NOS2 (**B**), or H3K9ac (**C**) in CD68$^+$ cells by immunofluorescence. In each panel, CD68 is depicted in red, the protein of interest in green, and the nuclei in blue. CD68$^+$ARG1$^+$ and CD68$^+$NOS2$^+$ cells are shown in yellow, and the presence of H3K9ac in CD68$^+$ cells is depicted in bright green/white. In A-C, the box in the low power image denotes the area of the higher power image. Scale bars, 100 μm.

In C, the open arrowheads indicate cells that are positive for CD68 and negative for H3K9ac; the solid arrowheads indicate cells that are positive for both CD68 and H3K9ac. Quantification was performed using ImageJ and shown in the right panels. *$P < 0.05$ for Odc^{mye} versus $Odc^{fl/fl}$ mice.